



Published in final edited form as:

J Proteome Res. 2017 September 01; 16(9): 3147–3157. doi:10.1021/acs.jproteome.7b00001.

The human regulatory protein Ki-1/57 is a target of SUMOylation and affects PML nuclear bodies formation

Ângela Saito¹, Edmarcia E. Souza², Fernanda C. Costa³, Gabriela V. Meirelles¹, Kaliandra A. Gonçalves¹, Marcos T. Santos⁴, Gustavo C. Bressan⁵, Mark E. McComb⁶, Catherine E. Costello⁶, Stephen A. Whelan⁶, Jörg Kobarg^{*,2}

Ângela Saito: angela.saito@lnbio.cnpem.br; Edmarcia E. Souza: edmarciaelisa@gmail.com; Fernanda C. Costa: ferccosta@gmail.com; Gabriela V. Meirelles: gabrielavm@gmail.com; Kaliandra A. Gonçalves: kaliandra.goncalves@lnbio.cnpem.br; Marcos T. Santos: marcos@onkos.com.br; Gustavo C. Bressan: gustavo.bressan@ufv.br; Mark E. McComb: mccomb@bu.edu; Catherine E. Costello: cecmsms@bu.edu; Stephen A. Whelan: sawhelan@bu.edu; Jörg Kobarg: jorgkoba@unicamp.br

¹Laboratório Nacional de Biociências (LNBio), Centro Nacional de Pesquisa em Energia e Materiais (CNPem), 13083-970, Campinas, SP, Brazil

²Faculdade de Ciências Farmacêuticas, Universidade Estadual de Campinas, Campinas, 13083-859, SP, Brazil

³Instituto de Física de São Carlos, Universidade de São Paulo, São Carlos, 13563-120, SP, Brazil

⁴ONKOS Molecular Diagnostics Inc, R&D Department, Ribeirão Preto, SP, Brazil

⁵Departamento de Bioquímica e Biologia Molecular, Universidade Federal de Viçosa (UFV), Viçosa, MG, Brazil

⁶Center for Biomedical Mass Spectrometry, Boston University School of Medicine, Boston, MA, USA

Abstract

Ki-1/57 is a nuclear and cytoplasmic regulatory protein first identified in malignant cells from Hodgkin's lymphoma. It is involved in gene expression regulation on both transcriptional and mRNA metabolism levels. Ki-1/57 belongs to the family of intrinsically unstructured proteins, undergoes phosphorylation by PKC and methylation by PRMT1. Previous characterization of its protein interaction profile by yeast two-hybrid screening showed that Ki-1/57 interacts with proteins of the SUMOylation machinery: the SUMO E2 conjugating enzyme UBC9 and the SUMO E3 ligase PIAS3, which suggested that Ki-1/57 could be involved with this process. Here we identified seven potential SUMO target sites (lysine residues) on Ki-1/57 sequence and observed that Ki-1/57 is modified by SUMO proteins *in vitro* and *in vivo*. FLAG-Ki-1/57 wild-type and mutant Lys to Arg proteins were overexpressed in HEK293T cells, immunoprecipitated with the antibody anti-FLAG and probed with anti-SUMO-1 or anti-SUMO-2/3. SUMOylation of Ki-1/57 occurred on lysines 213, 276 and 336. In transfected cells expressing FLAG-Ki-1/57 wild-type, its paralog FLAG-CGI-55 wild-type or their non-SUMOylated triple-mutants, the average

*Corresponding author: Jörg Kobarg. Universidade Estadual de Campinas, Rua Monteiro Lobato 255, Bloco F, Sala 03. CEP 13083-862, Campinas-SP, Brazil, Tel.: +55 19-3521 1443. jorgkoba@unicamp.br.

Supporting Information

The Supporting Information is available free of charge on the ACS Publications website at DOI: 10.1021/acs.jproteome.7b00001.

number of PML-nuclear bodies (PML-NBs) is reduced compared to the control cells not expressing the constructs. More interestingly, after treating cells with arsenic trioxide (As_2O_3) the mean number of PML-NBs is no more reduced when the non-SUMOylated triple-mutant Ki-1/57 is expressed, suggesting that the SUMOylation of Ki-1/57 has a role in the control of As_2O_3 -induced PML-NBs formation. A proteome-wide analysis of Ki-1/57 partners in the presence of either SUMO-1 or SUMO-2 suggests that the involvement of Ki-1/57 with regulation of gene expression is independent of the presence of either SUMO-1 or SUMO-2; however the presence of SUMO-1 strongly influences the interaction of Ki-1/57 with proteins associated to cellular metabolism maintenance and cell cycle.

Keywords

Ki-1/57; CGI-55; SUMOylation; posttranslational modifications; PML-NBs; arsenic trioxide

Introduction

Ki-1/57 (HABP4) is a regulatory protein first identified by the cross-reactivity of the CD30 antibody Ki-1 in malignant cells from Hodgkin lymphoma¹⁻³. Electron microscopic analyses demonstrated that Ki-1/57 is located in the cytoplasm, nuclear pores and in the nucleus, where it can frequently be found in association with nucleoli and other smaller nucleolar bodies⁴. Ki-1/57 is phosphorylated on serine and threonine residues by protein kinase C (PKC)^{5,6}, and methylated by protein arginine *N*-methyltransferase 1 (PRMT1)⁷.

Ki-1/57 has a paralog protein, CGI-55 (SERBP1), which was first identified as a PAI-1 mRNA binding protein (PAIRBP1)⁸. CGI-55 is also located in the cytoplasm and in the nucleus, where it can be found in the nucleoli and p80-coilin-positive coiled bodies⁹. Ki-1/57 and CGI-55 share 40.7% identity and 67.4% similarity¹⁰, and both have a conserved domain named hyaluronic acid binding (HABP4) domain¹¹. The so-called HABP4 domain is enriched with several positively charged amino acids, which may explain the initial report that Ki-1/57 has an activity of binding to negative-charged hyaluronan¹¹. In addition, Ki-1/57 and CGI-55 proteins have several RGG/RXR motifs which can act as RNA or other nucleic acid binding modules^{7,12,13}.

Several Ki-1/57 protein partners are directly or indirectly related to transcriptional regulation^{14,15}, while others are involved in mRNA metabolism, such as pre-mRNA splicing and translation^{6,7,12,16}. Moreover, a previous global transcriptome profile analysis performed after over-expressing Ki-1/57 revealed that these functional activities are related to cell proliferation and apoptosis control¹³.

Prior studies also showed the association of Ki-1/57 and CGI-55 with several proteins involved in the small ubiquitin-like modifier (SUMO) conjugation pathway, a reversible post-translational modification that regulates diverse cellular processes, including transcription, DNA repair, chromatin structure, cell-cycle progression and subcellular protein localization^{9,15,17-19}. In the process of SUMOylation, SUMO is covalently attached to a lysine residue in a $\Psi KX(D/E)$ sequence of a specific target protein, where Ψ is a large hydrophobic residue and X represents any amino acid. Four 11-kDa SUMO proteins can be

found in mammals, SUMO-1, -2, -3, and -4; the capacity to form polymeric chains through its lysine 11 is only known for SUMO-2/3, but not SUMO-1^{20–22}.

Both Ki-1/57 and CGI-55 interact with several proteins of PML nuclear bodies (PML-NBs) such as p53, DAXX, TOPORS, UBC9 and PIASy^{9,15,23}. PML-NBs are dynamic domains formed by PML proteins, which recruit protein partners in response to oxidative stress and interferon stimulation^{24–26}. SUMOylation has been shown as a key player in PML-NBs organization and biochemical functions²⁵. Upon arsenic trioxide (As₂O₃) treatment, PML oxidation leads to PML nucleation onto nuclear bodies (NBs), followed by recruitment to NBs of the SUMO E2 enzyme UBC9, which binds to PML and stimulates the SUMO-conjugation of PML. Then, the SUMOylated PML becomes a docking site for the association of partner proteins through multiple labile SUMO-SIM interactions. The SUMO-interacting motif (SIM) of the partner protein is able to interact to SUMOs covalently linked to PML, forming a polarized interaction and resulting in the retention of the partner within the NB core.

In this work, we demonstrate that the human protein Ki-1/57 and its paralog CGI-55 are modified by both SUMO-1 and SUMO-2 proteins. Our results suggest a possible involvement of both Ki-1/57 and CGI-55 in the control of PML-NBs formation, but only Ki-1/57 SUMOylation has a role in As₂O₃-induced PML-NBs formation control. The proteome-wide analyses performed suggest that the involvement of Ki-1/57 in gene expression control is independent of the presence of either SUMO-1 or SUMO-2, while SUMO-1 strongly influences the interaction of Ki-1/57 with cellular metabolism and cell cycle proteins. Together, our data show the SUMOylation of Ki-1/57 and suggest an involvement of this post-translational modification with the control of As₂O₃-induced PML-NBs formation.

Experimental Procedures

Plasmid Construction

The cDNA encoding full-length Ki-1/57 (1-413) in fusion with the N-terminal FLAG tag into pcDNA6 (pcDNA6-FLAG-Ki-1/57) has been previously described¹². Cloning Ki-1/57 as a C-terminal fusion to GST (GST-Ki-1/57) into pGEX-2TK has been described⁶. Point mutant derivatives of Ki-1/57 consisting of two double-mutants (K213R/K336R or K276R/K336R), and one triple mutant (K3R= K213R/K276R/K336R) were constructed using QuikChange™ Site-Directed Mutagenesis Kit (Stratagene) with the primers 5′-GCTTTTGACCAGAGAGGAAGGCGAGAATTTGAAAG-3′ (K213R sense, mutated codon underlined) and 5′-CTTTCAAATTCTCGCCTTCCTCTCTGGTCAAAGC-3′ (K213R antisense), 5′-GAGTCTCCAGCCAGAGTTCCTGAGTTGG-3′ (K276R sense, mutated codon underlined) and 5′-CCAACTCAGGAAGTCTGGCTGGAGACTC-3′ (K276R antisense), 5′-ACAGAGATGATATGGTAAGAGATGACTATGAGGACGATTCC-3′ (K336R sense, mutated codon underlined) and 5′-GGAATCGTCCTCATAGTCATCTTACCATATCATCTCTGT-3′ (K336R antisense). Mutants were sub-cloned into pcDNA6-FLAG. The cDNA encoding the isoform 1 of CGI-55 (1-408) was cloned in fusion with the N-terminal FLAG tag into the pcDNA6

(pcDNA6-FLAG-CGI-55) using BamHI-XhoI restrictions sites. A mutant of CGI-55 containing three lysines mutated to arginines (triple mutant, K3R= K102R/K228R/K281R) was synthesized, flanked by BamHI and XhoI restriction sites and cloned in fusion with the N-terminal FLAG tag into pcDNA6-FLAG (Genscript, USA). Full-length human SUMO-1, SUMO-2 and UBC9 cDNAs were PCR-amplified from HeLa cDNA library and cloned in fusion with the N-terminal Myc tag using BamHI-XhoI restrictions sites of pcDNA3.1/Hygro-Myc vector generating the constructs: pcDNA3.1-Myc-SUMO-1; pcDNA3.1-Myc-SUMO-2 and pcDNA3.1-Myc-UBC9.

Protein Expression and Purification

GST-Ki-1/57 was expressed in *Escherichia coli* BL21 strain by induction with 0.5 mM IPTG. Purification of lysate was performed using GST-Trap column (Amersham) and elution buffer containing 50 mM Tris-HCl pH 8,0; 50 mM NaCl; 0,1 mM EDTA; 20 mM reduced glutathione. The obtained GST- affinity purified fractions were pooled and dialyzed against the buffer: 50 mM Tris-HCl pH 8,0; 50 mM NaCl; 0,1 mM EDTA. The concentration of the recombinant protein was determined spectroscopically using the calculated extinction coefficient for the denatured proteins as described²⁷.

In vitro SUMOylation assay

For the *in vitro* SUMOylation assays, a SUMOylation Kit (BIOMOL) was used according to the manufacturer's instructions. GST-RanGAP1 protein provided by the kit and GST-Ki-1/57 were used at 2 nM concentration each. The control reactions were carried out in the absence of ATP. Reactions were analyzed by Western blot using rabbit polyclonal anti-SUMO-2/3 (1:1000 dilution - BIOMOL) or mouse monoclonal anti-Ki-1/57 (A26)².

Cell culture and transfections

HEK293T and HeLa cells were cultivated in high-glucose Dulbecco's modified Eagle's medium (DMEM, Sigma-Aldrich) supplemented with 10% fetal bovine serum (FBS, Invitrogen, South America), 100 U/ml penicillin and 100 µg/ml streptomycin (Invitrogen) at 37 °C and 5% CO₂ atmosphere. Transient transfections in HEK293T cells were performed using the calcium phosphate method¹² or the linear 25 kDa polyethylenimine (PEI, Polysciences)¹³. HeLa cells were transfected with Fugene 6 Transfection Reagent (Promega) according to the manufacturer's instructions.

Immunoprecipitation assay for detection of SUMOylated proteins by Western blot

After 48 h of transfection, cells were washed in ice-cold PBS supplemented with 10 mM *N*-ethylmaleimide (NEM, Sigma-Aldrich), lysed in buffer containing PBS, 1% SDS, 5 mM EDTA, 5 mM EGTA, 10 mM NEM and complete protease inhibitor cocktail (Roche). After brief sonication, 50 mM DTT was added to the cell lysates, and the mixture was boiled for 95 °C and diluted 1:3 in cold RIPA dilution buffer (20 mM phosphate buffer pH 7.4, 150 mM NaCl, 1% Triton X-100, 0.5% sodium deoxycholate, 5 mM EDTA, 5 mM EGTA, 10 mM NEM and complete protease inhibitor set). Lysates were cleared at 16000 × *g* at 4 °C for 20 min²⁸. Protein concentrations were determined using the BCA Protein Assay Reagent Kit (Thermo Scientific). The cleared lysates were incubated with a homemade rabbit

polyclonal anti-Ki-1/57 or anti-CGI-55 coupled to protein A-Sepharose 4 fast-flow beads (GE Healthcare), or mouse monoclonal anti-FLAG M2 (Sigma-Aldrich) coupled to protein G-Sepharose 4 fast flow beads (GE Healthcare) at 4 °C for 16 h. Beads were recovered and washed three times in lysis buffer before elution of immunoprecipitated proteins in sample buffer. The eluates were analyzed by Western blot, using rabbit polyclonal anti-SUMO-2 (1:1000 dilution; Abcam), rabbit polyclonal anti-SUMO-1 (1:500 dilution, Abgent) and mouse monoclonal anti-FLAG M2 (1:5000 dilution; Sigma-Aldrich). Membranes were incubated with the respective horseradish peroxidase-conjugated secondary (1:5000 dilution) for 1 h, washed and developed by chemiluminescence using Amersham ECL Prime Western Blotting Detection Reagent.

Immunofluorescence and image analysis

HeLa cells were cultivated onto coverslips, transfected with the constructs, and treated or not with 2 μ M of As₂O₃ (Sigma-Aldrich) for 90 min. The cells were fixed and permeabilized for immunofluorescence in 3.7% formaldehyde solution (Sigma-Aldrich) containing 0.2% Triton X-100 in PBS 1x at room temperature for 20 min. The fixed specimens were quenched with 7.5 mg/mL glycine following rehydration in PBS at room temperature for 5 min, and blocked in PBS-AT (3% BSA, 0.5% Triton X-100 in PBS 1x) at room temperature for 30 min. The cells were incubated for 1 h at room temperature in primaries antibodies diluted in PBS-AT: mouse anti-PML (PG-M3; Santa Cruz Biotechnology; sc-966, 1:400 dilution); goat anti-P53 (C-19; Santa Cruz Biotechnology; sc-1311, 1:500 dilution); rabbit anti-FLAG (F7425; Sigma-Aldrich, 1:1000 dilution); mouse anti-FLAG (F1804; Sigma-Aldrich, 1:1000 dilution). Primary antibodies were removed by washing with PBST-AT and incubated for 40 min with the related secondary antibodies diluted in PBS-AT: chicken anti-mouse Alexa Fluor 488 (A21200; Life Technologies); chicken anti-goat Alexa Fluor 488 (A21467; Life Technologies); donkey anti-rabbit Alexa Fluor 546 (A10040; Life Technologies); chicken anti-mouse Alexa Fluor 647 (A21463; Life Technologies); donkey anti-goat Alexa Fluor 546 (A11056; Life Technologies); chicken anti-rabbit Alexa Fluor 488 (A21441; Life Technologies). The cells were stained with Hoescht 33258 (Sigma-Aldrich) to visualize nuclei. After rinsing in PBS 1x, cells were mounted in ProLong Gold mounting media (Life Technologies), followed by confocal microscopy imaging.

From the coverslips, a series of Z-stack images of interphase cells was captured from 0.35 μ m thick sections using a Confocal Laser Scanning Microscope SP8 (Leica) or from 0.7 μ m thick sections using a Carl Zeiss LSM 780 confocal microscope equipped with objective Plan-Apochromat 63x/1.40 Oil DIC M27. The entire fixed cell volume imaged was processed for three-dimensional (3D) using Imaris (Bitplane). For dot measurement, cells were imaged using identical microscope settings within each experimental set. PML dots per cell were identified after 3D reconstruction by the Spots function on Imaris (Bitplane) using a fixed spot size of 0.5 μ m (the measured average XY diameter of cell bodies). The analyses were performed using identical threshold settings. P-values were generated by unpaired t-test using Prism 6 (GraphPad). P<0.05 was considered as statistically significant.

Immunoprecipitation followed by Liquid chromatography-tandem MS (IP-LC-MS/MS) and data analysis

Cells were transfected as following: pcDNA6-FLAG-Ki-1/57, pcDNA3.1-Myc-UBC9 and pcDNA3.1-Myc-SUMO-1 or pcDNA3.1-Myc-SUMO-2; pcDNA6-FLAG-CGI-55, pcDNA3.1-Myc-UBC9 and pcDNA3.1-Myc-SUMO-1 or pcDNA3.1-Myc-SUMO-2; pcDNA-FLAG empty vector, pcDNA3.1-Myc-UBC9 and pcDNA3.1-Myc-SUMO-1 or pcDNA3.1-Myc-SUMO-2. All transfections were performed in duplicate using the linear 25 KDa PEI reagent (Polysciences). Then, 48 h after transfection, cells were washed with ice-cold PBS 1x containing 10 mM NEM and harvested by trypsinization. The pellets were incubated in lysis buffer (1% Triton X-100, 5 mM EDTA, 20 mM NEM, 1 $\mu\text{g}/\mu\text{L}$ DNase I, and protease inhibitors cocktail diluted in PBS 1x) for 20 min at 4 °C. Cells were maintained on ice and sonicated at 20% power for 10 seconds with 1 second intervals. Sequentially the lysates were cleared by centrifugation and incubated overnight with mouse anti-FLAG M2 AffinityGel (Sigma-Aldrich). Beads were washed twice with wash buffer (50 mM Tris-HCl, 150 mM NaCl, pH 7.4), once with PBS 1x, followed by resuspension in 25 μL of 6 M urea. FLAG-immunoprecipitated proteins were reduced, alkylated and in-solution digested by Trypsin Gold as described in manufacturer's protocol (Promega). The resulting peptide mixtures were submitted to liquid chromatography –mass spectrometry analysis (LC–MS) using a nano-Acquity UPLC nano-capillary high-performance LC system (Waters Corp., Milford, MA, USA) coupled to a Q Exactive hybrid quadrupole-Orbitrap mass spectrometer (Thermo Fisher Scientific) equipped with a TriVersa NanoMate ion source (Advion, Ithaca, NY, USA). Sample concentration and desalting were performed online using a nanoAcquity UPLC trapping column (180 μm \times 20 mm, packed with 5- μm , 100- \AA Symmetry C18 material; Waters) at a flow rate of 15 $\mu\text{L}/\text{min}$ for 1 min. Separation was accomplished on a nanoAcquity UPLC capillary column (150 μm \times 100 mm, packed with 1.7- μm , 130- \AA BEH C18 material; Waters). A linear gradient of A and B buffers (buffer A: 1.5% ACN and 0.1% FA; buffer B: 98.5% ACN and 0.1% FA) from 2 to 40% buffer B over 80 min was used at a flow rate of 0.5 $\mu\text{L}/\text{min}$ to elute peptides into the mass spectrometer. Columns were washed and re-equilibrated between LC-MS experiments. Electrospray ionization was carried out at 1.65 kV using the NanoMate, with the Q Exactive heated transfer capillary set to 250 °C. Mass spectra were acquired in the positive-ion mode over the range m/z 400–2000 at a resolution of 70,000 (full width at half maximum at m/z 400; \sim 1 spectrum/s) and AGC target of $>3 \times e^6$. Mass accuracy after internal calibration was within 1 ppm. MS/MS spectra were acquired using a Top10 method by sampling the 10 most abundant, multiply charged species in each mass spectrum with a resolution of 17,500 and signal intensities $>2 \times e^5$ NL, using HCD with MS/MS collision energies set at 3 stepped NCE (15 v, 25 v, 35 v), nitrogen as the collision gas, and MS/MS spectra acquisition over a scan range of m/z 200 to 2000, dependent on the precursor ion. Underfill ratio was 1% with an intensity threshold of $2.5 e^4$, and an apex trigger of 2 to 4 seconds. Charge exclusion was set for 1 and >8 and dynamic exclusion was set such that MS/MS for each precursor ion species was excluded 10.0 seconds post-acquisition. All spectra were recorded in profile mode for further processing and analysis.

MS and MS/MS data analysis was carried out using both Proteome Discoverer (PD) 1.4 SEQUEST software (Thermo Fisher Scientific) and accessing an in-house Mascot 2.3 server

(Matrix Science, London, UK) through the PD1.4 software. The MS/MS data were searched against the UniProt HUMAN_2015_02_10.fasta database amino acid sequence database (89775 entries) for protein/peptide identification. The PD 1.4 and Mascot searches were set up with precursor intensity node, full tryptic peptides with a maximum of 2 missed cleavage sites with carbamidomethyl cysteine and oxidized methionine included as variable modifications. Percolator was set at maximum delta Cn of 0.05, decoy database search of target FDR set at (strict) 0.01, target FDR (relaxed) at 0.05 and validation based on the q-Value. The precursor mass tolerance was set to 10 ppm for Q Exactive orbitrap data, and the maximum fragment mass error was 0.02 Da. The PD1.4 searches were uploaded into Scaffold 4.4.8. Scaffold filters were set for a minimum of 1.0% FDR for protein threshold, minimum of 5 peptides and a minimum of 0.1% FDR for peptides threshold. Protein clustering and decoy database was used (1034 proteins identified and 136832 spectra, protein 0.5% decoy FDR; minimum of 2 peptides yielded 2051 proteins identified from 142,753 spectra, protein 0.7% decoy FDR). Scaffold quantitation analysis was calculated through fold change by category based on total precursor intensity and use of normalization²⁹. In order to increase the confidence in the identification of obtained proteins we generated the final list of proteins following selection criteria: (i) fold change >2; (ii) presence of exclusive peptides after co-expression of Ki-1/57 or CGI-55 and either SUMO-1 or SUMO-2 (those proteins that were present in the negative controls pcDNA3.1-Myc-SUMO-1 or pcDNA3.1-Myc-SUMO-2 of anti-FLAG affinity purifications were excluded from the list); (iii) a minimum number of at least two unique peptides present in the duplicate experiments. Next, to avoid the selection of nonspecific interactors from affinity purification using anti-FLAG, we compared the generated list of co-precipitated proteins with the Contaminant Repository for Affinity Purification, CRAPome (<http://www.crapome.org/>).

***In silico* PPI analysis**

The retrieved Ki-1/57 (HABP4) and CGI-55 (SERBP1) interacting partners from IP-MS/MS in the presence of either SUMO-1 or SUMO-2 were integrated in interaction networks using the Integrated Interactome System (IIS)³⁰. The enriched biological processes from the Gene Ontology (GO, <http://www.geneontology.org/>) database were calculated in each network using the hypergeometric distribution³⁰. The interaction networks were visualized using Cytoscape 2.8.3 software³¹.

Results

Ki-1/57 possesses predicted SUMOylation sites in its amino acid sequence and is modified by SUMO-2/3 *in vitro*

In order to investigate whether human Ki-1/57 has predicted SUMOylation sites, the Ki-1/57 amino acid sequence was analyzed through the web-available SUMOplot™ tool (Figure 1A). Seven potential SUMO conjugation sites were identified, in which the lysines 213, 276 and 336 were found as the most likely sites for SUMOylation, with a score higher than 67%. By comparing the scores with those of other known SUMOylated proteins, human Ki-1/57 seemed to be a potential target of SUMOylation. To study this hypothesis, recombinant GST-Ki-1/57 was used as substrate protein for *in vitro* SUMOylation assay (Figure 1B). The

reaction was performed in the presence of ATP, SUMO E1 and E2 enzymes, SUMO-2 or SUMO-3 proteins, followed by Western blot using antibodies against SUMO-2/3. As observed in Figure 1B, the slowest-migrating high molecular weight bands show that GST-Ki-1/57 is modified by SUMO-2 and -3 proteins.

Ki-1/57 and CGI-55 are conjugated with SUMO-1 or SUMO-2 proteins *in vivo*

Next, in order to verify whether human Ki-1/57 is also a SUMOylated protein *in vivo*, FLAG-tagged Ki-1/57 was transiently expressed with the SUMO-conjugating enzyme E2 UBC9 fused to Myc (Myc-UBC9) and SUMO-1 or SUMO-2 proteins (Myc-SUMO-1 or Myc-SUMO-2, respectively) in HEK293T cells. FLAG-Ki-1/57 was immunoprecipitated, followed by Western blot analyses using anti-FLAG, anti-SUMO-1 and anti-SUMO-2 antibodies. As shown in Figure 2A and 2B, immunoprecipitated FLAG-Ki-1/57 was detected with anti-SUMO-1 and anti-SUMO-2 antibodies, respectively, indicating that human Ki-1/57 is a SUMOylated protein *in vivo*.

CGI-55 also contains several potential SUMOylated motifs (Supplemental Figure S-1) and, in order to verify whether CGI-55 is also modified by both SUMO-1 and SUMO-2 under normal culture conditions, FLAG-tagged CGI-55 was transiently expressed with Myc-UBC9, and Myc-SUMO-1 or Myc-SUMO-2 proteins. Immunoprecipitation and Western blot showed that CGI-55 is highly modified by both SUMO-1 and SUMO-2 proteins under non-stressed culture conditions (Figure 2B and 2C, respectively).

Previously, a global SUMOylation study by mass spectrometry identified CGI-55 containing three lysine residues modified by SUMO-2³². In order to verify whether these lysine residues are also modified by SUMO-1 *in vivo*, we expressed the isoform 1 of CGI-55 containing these three lysines mutated to arginines (triple mutant: K102R/K228R/K281R) along with Myc-SUMO-1 and Myc-UBC9 in HEK293T cells. The FLAG-tagged wild-type and triple mutant constructs were FLAG-immunoprecipitated and subjected to Western blot analysis with anti-FLAG, which showed that the triple mutant is not more modified by SUMO-1 (Figure 2D).

Site-directed mutagenesis was also approached for Ki-1/57, in which the lysines residues with the highest score in SUMOplot™ analysis (Figure 1A) have been changed to arginine to preserve the positive amino acid charge. As shown in Figure 3A, SUMO-1 modification was significantly weaker but could still be detected in the two Ki-1/57 double mutants K213R/K336R or K276R/K336R. However, SUMO-1 modification was no longer detectable in the Ki-1/57 triple mutant (K3R= K213R/K276R/K336R). In summary, these data indicate that the lysines 213, 276 and 336 are all acceptor sites for SUMO conjugation in Ki-1/57. The Ki-1/57 triple mutant was also tested for the SUMO-2 modification *in vivo*. As shown in Figure 3B, only the wild-type protein but not the triple mutant is modified by SUMO-2 (Figure 3B).

Ki-1/57 and CGI-55 overexpression affects PML-NBs formation

The observation that several Ki-1/57 and CGI-55-interacting proteins (p53, DAXX, TOPORS, UBC9, PIASy) can localize to PML nuclear bodies (PML-NBs) and can be modified by SUMO proteins led us to investigate a possible role of Ki-1/57 and CGI-55 in

PML-NBs formation and distribution. For that, HeLa cells were transiently transfected with plasmids for the expression of FLAG-Ki-1/57 wild-type, FLAG-Ki-1/57 triple mutant (K3R: K213R/K276R/K336R), FLAG-CGI-55 wild-type or FLAG-CGI-55 triple mutant (K3R: K102R/K228R/K281R), followed by immunolabeling against PML and FLAG (Figure 4A). PML-NBs were counted in maximum-intensity Z projections of individual cells. We found that under untreated conditions the expression of Ki-1/57, CGI-55 or their triple mutants significantly reduced the PML-NBs number compared to the control cells not expressing the constructs (Figure 4B).

Arsenic trioxide (As_2O_3) has been shown to induce PML oxidation, UBC9 recruitment to NBs, and to enhance the number of PML-NBs²⁵. To increase the PML-NBs formation, cells were treated with arsenic trioxide after transfection with the constructs. Under this condition, we observed that the mean number of PML-NBs was significantly decreased when Ki-1/57 wild-type, CGI-55 wild-type or CGI-55 triple mutant were expressed compared to the control cell not expressing these proteins. Interestingly, no significant reduction in PML-NBs number was observed in cells expressing Ki-1/57 triple mutant (K3R) compared to the control cell. Therefore, this finding suggests that the SUMOylation of Ki-1/57 has a role in the control of As_2O_3 -induced PML-NBs formation (Figure 4B).

In cells presenting higher levels of expression of Ki-1/57, CGI-55 or their triple mutants, we observed an increase in the soluble PML, as seen by its diffuse distribution in the nucleus and eventually in the cytoplasm, which suggests that PML distribution was affected. This effect was similar in the presence of As_2O_3 -induced stress (Supplemental Figure S-2).

A proteome-wide view of Ki-1/57 and CGI-55 interacting partners in the presence of either SUMO-1 or SUMO-2

To investigate whether the modification of Ki-1/57 and CGI-55 by either SUMO-1 or SUMO-2 could change their interacting partners and their involvement in different biological processes, we performed a proteome-wide analysis after the co-expression of Ki-1/57 and CGI-55 with either SUMO-1 or SUMO-2. FLAG-immunoprecipitated proteins were in-solution digested by trypsin, and the resulting peptide mixtures were analyzed by LC-MS/MS. In the presence of SUMO-1, Ki-1/57 co-precipitated 68 proteins, in contrast to only 29 proteins when SUMO-2 was co-expressed (Supplemental Table S-1). The resulting difference between affinity purification-MS data for the Ki-1/57 immunoprecipitation with SUMO-1 or SUMO-2 is not a result from the different expression level of Ki-1/57, since the target protein was immunoprecipitated in the same quantities in the presence of either SUMO-1 or SUMO-2 paralogs (Supplemental Figure S-3). In order to better investigate the pathways among the protein complexes formed when either SUMO-1 or SUMO-2 were expressed, we performed biological processes analyses based on Gene Ontology (GO) annotation (Figure 5). Several biological processes were enriched when Ki-1/57 and SUMO-1 were co-expressed: regulation of transcription, RNA splicing, translation, ribosome biogenesis, mitotic cell cycle, apoptotic process and DNA repair (Figure 5A; Supplemental Table S-2). Interestingly, SUMO-2 expression with Ki-1/57 led to an enrichment of only a few biological processes: those related to gene expression regulation as

transcription, RNA splicing and translation and the process of telomere maintenance (Figure 5B; Supplemental Table S-3).

In the case of CGI-55, its co-expression with SUMO-1 or SUMO-2 retrieved 101 and 105 proteins, respectively (Supplemental Table S-1). GO biological processes analyses showed the enrichment of the terms related to regulation of gene expression, as transcription, RNA splicing and translation, ribosome biogenesis, apoptotic process and mitosis for the presence of either SUMO-1 or SUMO-2 when CGI-55 was co-expressed (Figure 5C and 5D; Supplemental Table S-4 and S-5).

Previously Ki-1/57 had been shown to interact with translational machinery proteins¹⁶. Here we found FMRP co-precipitated with Ki-1/57 when SUMO-1 was expressed, FXR2 and several mitochondrial ribosomal proteins (MRPS and MRPL) formed complexes with Ki-1/57 when either SUMO-1 or SUMO-2 were co-expressed. In the presence of SUMO-1, but not SUMO-2, Ki-1/57 co-precipitated several proteins related to ribosome biogenesis as: proteins containing GTPase activity GTPBP4, GNL2, and GTPBP10, and proteins implicated in the regulation of the cell cycle BOP1, SURF6, and MRTO4. BOP1 and MRTO4 have been associated to cellular adaptation to stresses, affecting cellular metabolism and cell cycle regulation³³⁻³⁵. These data not only confirmed previous studies, but also revealed novel interacting partners related to translational regulation and biogenesis of ribosome along with possibilities of controlling these proteins functions through SUMOylation.

Discussion

In this study, we investigated the SUMOylation of the human regulatory protein Ki-1/57 and its possible role for the function of Ki-1/57. The earliest indication that Ki-1/57 and its paralog protein, CGI-55, could be post-translationally modified by SUMO proteins emerged with the discovery that these proteins are associated to proteins of the SUMOylation machinery^{9,15}. Yeast two-hybrid assays revealed that the N-terminal region of Ki-1/57 interacts with the SUMO E2 enzyme UBC9 and the C-terminal region interacts with the SUMO E3 enzymes PIAS3 and TOPORS¹⁵. Further, CGI-55 was shown to interact with the SUMO E1 enzyme subunit UBA2 and the SUMO E3 enzymes PIAS-1, -3, -y and TOPORS⁹. During the process of SUMOylation, the attachment of SUMO to a target protein is mediated by a sequential cascade of reactions: the energy-dependent activation of mature SUMO protein by SUMO-activating enzyme E1 (formed by a heterodimer AOS1/UBA2), transfer of SUMO from E1 to UBC9, which catalyze conjugation to a substrate, resulting in the formation of an isopeptide bond between the C-terminal carboxyl group of the SUMO and an ϵ -amino group of a substrate acceptor lysine residue^{17,20}.

Here, we showed that Ki-1/57 contains several predicted SUMOylation motifs, and demonstrated the modification of human Ki-1/57 and CGI-55 by either SUMO-1 or SUMO-2 proteins *in vivo*. Ki-1/57 has been previously identified as modified by SUMO-1 during the mitotic phase of cell cycle in a mass spectrometry study using *Xenopus* egg extract³⁶. In addition, through *in vitro* SUMOylation assay, our group has showed that the modification of Ki-1/57 by SUMO-1 can be enhanced by the presence of STC-1, a SUMO

E3 ligase protein³⁷. The paralog CGI-55 has been shown to conjugate to SUMO-2 in a systematic study on SUMO modifications in response to heat shock³⁸. Also, a study on the identification of global SUMOylation sites by mass spectrometry identified the second isoform of CGI-55 (Q8NC51-2) as containing three SUMO-2 target sites, lysines 102, 222 and 275 in HeLa cells under control, MG132, heat-shock and PR619-treated cells³². Here, we showed that the first isoform of CGI-55 (Q8NC51) containing three mutations, on lysines 102, 228 and 281, is indeed no more modified by SUMO-1.

In order to identify the SUMOylated motifs in Ki-1/57, we performed site-directed mutagenesis of its predicted SUMOylated lysines. The wild-type and mutants containing two or three different combinations of mutations in Ki-1/57 were transiently transfected in HEK293T cells and immunoprecipitated by anti-FLAG antibody. SUMOylation was assessed by using antibodies against SUMO-1 or SUMO-2 with the immunoprecipitated protein. We could identify three SUMOylated lysines (K3R= K213/K276/K336) in Ki-1/57 protein. Since Ki-1/57 and CGI-55 are SUMOylated and they may interact with known SUMO E3 ligases, such as TOPORS and PIAS proteins, it would be possible to speculate whether these E3 enzymes work enhancing the SUMOylation of Ki-1/57 and CGI-55.

Post-translational modifications of proteins have been shown to regulate their functions, properties and subcellular localizations by adding more flexibility and/or modulating their capacity of interaction to other protein or DNA/RNA. Protein-protein interaction and the subcellular localization of Ki-1/57 have been previously shown to be regulated by its post-translational modifications. Ki-1/57 is phosphorylated on serine and threonine residues by PKC upon activation of Hodgkin's lymphoma analogous cell line L540 with the PKC-activator PMA. Under these conditions, the interaction between Ki-1/57 and the adaptor protein RACK1 (receptor of activated kinase 1) is abolished, resulting in Ki-1/57 translocation from the nucleus to the cytoplasm⁶. Also, Ki-1/57 interacts with and is methylated by protein arginine N-methyltransferase 1 (PRMT1)⁷. The methylation status of Ki-1/57 is important for its localization to small nuclear bodies. Under normal cellular conditions, Ki-1/57 can partially localize to nuclear speckles, which is known structures for storage of splicing factors. Upon treatment with the methylation inhibitor Adox, Ki-1/57 was found to localize to the nucleoli, where ribosomal biogenesis and maturation take place and to Cajal-bodies and GEMS, known important sites for spliceosomal and non-spliceosomal snRNP biogenesis, maturation and recycling³⁹. The subcellular localization of CGI-55 is also regulated by its methylation status. In cells treated with Adox, CGI-55 was found to localize predominately to the nucleus⁴⁰.

Interestingly, we have previously found that both Ki-1/57 and CGI-55 interact with several PML nuclear bodies (PML-NBs) proteins such as p53, DAXX, TOPORS, UBC9 and PIASy^{9,15,23}. Here, we performed confocal microscopy to analyze PML-NBs formation and distribution when Ki-1/57, CGI-55 or their triple mutants (K3R) were expressed in HeLa cells under normal conditions or As₂O₃-induced oxidative stress. PML-NBs were observed in punctuated nuclear bodies in the nucleus. Cells expressing Ki-1/57, CGI-55 or their triple mutants presented a reduced number of PML-NBs under untreated conditions. However, upon As₂O₃ treatment, the expression of Ki-1/57 triple mutant failed to reduce the mean number of PML-NB as the wild-type Ki-1/57 did. This result suggests that the

SUMOylation of Ki-1/57 may be involved in antioxidant mechanisms or cellular adjustments to oxidative stress.

In addition, we noticed that in cells containing higher expression levels of Ki-1/57, CGI-55 or their triple mutants (K3R) a rearrangement of PML-NBs occurred, as observed by an apparent increase in the soluble PML and reduced number of PML-NBs. Changes in the PML-NBs rearrangement with increased PML in a nucleoplasmic diffusible form has been described after UVC irradiation of human cells^{41,42} and shown to occur in a p53-dependent fashion. It was suggested that p53 participates of the redistribution of PML protein from PML-NBs to sites of repair of UVC-induced DNA damage⁴². Previously, Ki-1/57 was shown to interact with p53 and reduce its transcriptional activity¹⁵. Although the exact mechanism by which the action of Ki-1/57 in the PML redistribution is not explained with our data, the fact that Ki-1/57 is involved in gene expression regulation and is associated with p53 may be a way by which Ki-1/57 acts in the PML redistribution.

SUMOylation can alter different cellular processes depending on whether the substrate is conjugated by either SUMO-1 or SUMO-2/3, possibly because the functional properties of SUMO proteins may mediate distinct protein-protein interactions. SUMO proteins interact with hydrophobic domains, flanked by acid and/or serine residues, called the SUMO-interacting Motif (SIM). In this context, the covalent modification of a substrate by SUMO may provide interacting sites for other protein through SIM^{20,43}.

In order to study whether the modification of Ki-1/57 and CGI-55 by either SUMO-1 or SUMO-2 could change their interacting partners and their involvement in different biological processes, we performed a proteome-wide view of Ki-1/57 and CGI-55 when either SUMO-1 or SUMO-2 were co-expressed. We observed that the expression of SUMO-1 with Ki-1/57 or the expression of CGI-55 with either SUMO-1 or SUMO-2 retrieved interacting proteins related to regulation of transcription, RNA splicing, translation, ribosome biogenesis, apoptotic process, and mitosis. However, SUMO-2 expression with Ki-1/57 led to an enrichment of only a few biological processes, particularly, those related to the control of gene expression as transcription, RNA splicing and translation and related to telomere maintenance. These data may mean that the modification of Ki-1/57 by SUMO-2 blocks its interaction to others proteins, or SUMO-1 modification of Ki-1/57 or its partners increases its protein-protein interaction surfaces, thereby allowing a higher number of Ki-1/57 partners to interact with it via SUMO-1.

In summary, we showed that the paralogs Ki-1/57 and CGI-55 are SUMOylated proteins, and independently of their SUMOylation status, both Ki-1/57 and CGI-55 may be involved in the control of PML-NBs formation under untreated conditions. However, the SUMOylated form of Ki-1/57 showed to be important for the control of PML-NB formation under oxidative stress-induced conditions. We also showed that the modification of Ki-1/57 by SUMO-1 or CGI-55 by SUMO-1 or SUMO-2 is associated to several biological processes (regulation of transcription, RNA splicing, translation, ribosome biogenesis, mitotic cell cycle and apoptotic process), but SUMO-2-modified Ki-1/57 is strongly associated with biological processes related to the control of gene expression (transcription, splicing and translation) and telomere maintenance. Therefore, differences in SUMOylation,

phosphorylation and methylation activities seem to specify the functional role of Ki-1/57 and CGI-55, both associated with multiple aspects of gene expression regulation in human cells. These findings certainly help us to better understand how these regulatory proteins work under normal or stressed conditions.

Supplementary Material

Refer to Web version on PubMed Central for supplementary material.

Acknowledgments

We thank to Maria Eugenia Camargo for technical assistance, Laboratory of Biological Imaging at LNBio for confocal images using TCS SP8 Leica Microscope, National Institute of Science and Technology on Photonics Applied to Cell Biology (INFABIC, UNICAMP) for imaging support. INFABIC is co-funded by Fundação de Amparo a Pesquisa do Estado de São Paulo (FAPESP) (08/57906-3) and Conselho Nacional de Desenvolvimento Científico e Tecnológico (CNPq) (573913/2008-0). This work was financially supported by Fundação de Amparo à Pesquisa do Estado de São Paulo (FAPESP, grant 2014/21700-3). SAW, MEM and CEC are supported by NHLBI Contract HHSN268201000031C and NIH grant P41 GM104603.

References

1. Hansen H, Lemke H, Bredfeldt G, Könnecke I, Havsteen B. The Hodgkin-Associated Ki-1 Antigen Exists in an Intracellular and a Membrane-Bound Form. *Biol Chem Hoppe Seyler*. 1989; 370:409–416. [PubMed: 2545229]
2. Kobarg J, Schnittger S, Fonatsch C, Lemke H, Bowen MA, Buck F, Hansen HP. Characterization, mapping and partial cDNA sequence of the 57-kD intracellular Ki-1 antigen. *Exp Clin Immunogenet*. 1997; 14(4):273–280. [PubMed: 9523163]
3. Schwab U, Stein H, Gerdes J, Lemke H, Kirchner H, Schaadt M, Diehl V. Production of a monoclonal antibody specific for Hodgkin and Sternberg–Reed cells of Hodgkin’s disease and a subset of normal lymphoid cells. *Nature*. 1982; 299(5878):65–67. [PubMed: 7110326]
4. Rohde D, Hansen H, Hafner M, Lange H, Mielke V, Hansmann ML, Lemke H. Cellular localizations and processing of the two molecular forms of the Hodgkin-associated Ki-1 (CD30) antigen. The protein kinase Ki-1/57 occurs in the nucleus. *Am J Pathol*. 1992; 140(2):473–482. [PubMed: 1310832]
5. Hansen H, Bredfeldt G, Havsteen B, Lemke H. Protein kinase activity of the intracellular but not of the membrane-associated form of the KI-1 antigen (CD30). *Res Immunol*. 1990; 141(1):13–31. [PubMed: 2161115]
6. Nery FC, Passos DO, Garcia VS, Kobarg J. Ki-1/57 interacts with RACK1 and is a substrate for the phosphorylation by phorbol 12-myristate 13-acetate-activated protein kinase C. *J Biol Chem*. 2004; 279(12):11444–11455. [PubMed: 14699138]
7. Passos DO, Bressan GC, Nery FC, Kobarg J. Ki-1/57 interacts with PRMT1 and is a substrate for arginine methylation. *FEBS J*. 2006; 273(17):3946–3961. [PubMed: 16879614]
8. Heaton JH, Dlakic WM, Dlakic M, Gelehrter TD. Identification and cDNA Cloning of a Novel RNA-binding Protein That Interacts with the Cyclic Nucleotide-responsive Sequence in the Type-1 Plasminogen Activator Inhibitor mRNA. *J Biol Chem*. 2001; 276(5):3341–3347. [PubMed: 11001948]
9. Lemos TA, Kobarg J. CGI-55 Interacts With Nuclear Proteins and Co-Localizes to p80-Coilin Positive-Coiled Bodies in the Nucleus. *Cell Biochem Biophys*. 2006; 44:463–474. [PubMed: 16679534]
10. Lemos TA, Passos DO, Nery FC, Kobarg J. Characterization of a new family of proteins that interact with the C-terminal region of the chromatin-remodeling factor CHD-3. *FEBS Lett*. 2003; 533:14–20. [PubMed: 12505151]

11. Huang L, Grammatikakis N, Yoneda M, Banerjee SD, Toole BP. Molecular characterization of a novel intracellular hyaluronan-binding protein. *J Biol Chem*. 2000; 275(38):29829–29839. [PubMed: 10887182]
12. Bressan GC, Quaresma AJC, Moraes EC, Manfiolli AO, Passos DO, Gomes MD, Kobarg J. Functional association of human Ki-1/57 with pre-mRNA splicing events. *FEBS J*. 2009; 276(14):3770–3783. [PubMed: 19523114]
13. Costa FC, Saito A, Gonçalves KA, Vidigal PM, Meirelles GV, Bressan GC, Kobarg J. Ki-1/57 and CGI-55 ectopic expression impact cellular pathways involved in proliferation and stress response regulation. *Biochim Biophys Acta*. 2014; 1843(12):2944–2956. [PubMed: 25205453]
14. Kobarg CB, Kobarg J, Crosara-Alberto DP, Theizen TH, Franchini KG. MEF2C DNA-binding activity is inhibited through its interaction with the regulatory protein Ki-1/57. *FEBS Lett*. 2005; 579(12):2615–2622. [PubMed: 15862299]
15. Nery FC, Rui E, Kuniyoshi TM, Kobarg J. Evidence for the interaction of the regulatory protein Ki-1/57 with p53 and its interacting proteins. *Biochem Biophys Res Commun*. 2006; 341(3):847–855. [PubMed: 16455055]
16. Gonçalves, K de A; Bressan, GC; Saito, A; Morello, LG; Zanchin, NIT; Kobarg, J. Evidence for the association of the human regulatory protein Ki-1/57 with the translational machinery. *FEBS Lett*. 2011; 585(16):2556–2560. [PubMed: 21771594]
17. Gill G. SUMO and ubiquitin in the nucleus: different functions, similar mechanisms? *Genes Dev*. 2004; 18(17):2046–2059. [PubMed: 15342487]
18. Hannoun Z, Greenhough S, Jaffray E, Hay RT, Hay DC. Post-translational modification by SUMO. *Toxicology*. 2010; 278(3):288–293. [PubMed: 20674646]
19. Hay RT. SUMO: a history of modification. *Mol Cell*. 2005; 18(1):1–12. [PubMed: 15808504]
20. Geiss-Friedlander R, Melchior F. Concepts in sumoylation: a decade on. *Nat Rev Mol Cell Biol*. 2007; 8(12):947–956. [PubMed: 18000527]
21. Johnson ES. Protein modification by SUMO. *Annu Rev Biochem*. 2004; 73:355–382. [PubMed: 15189146]
22. Rodriguez MS, Dargemont C, Hay RT. SUMO-1 conjugation in vivo requires both a consensus modification motif and nuclear targeting. *J Biol Chem*. 2001; 276(16):12654–12659. [PubMed: 11124955]
23. Van Damme E, Laukens K, Dang TH, Van Ostade X. A manually curated network of the PML nuclear body interactome reveals an important role for PML-NBs in SUMOylation dynamics. *Int J Biol Sci*. 2010; 6(1):51–67. [PubMed: 20087442]
24. Bernardi R, Pandolfi PP. Structure, dynamics and functions of promyelocytic leukaemia nuclear bodies. *Nat Rev Mol Cell Biol*. 2007; 8(12):1006–1016. [PubMed: 17928811]
25. Sahin U, Ferhi O, Jeanne M, Benhenda S, Berthier C, Jollivet F, Niwa-Kawakita M, Faklaris O, Setterblad N, de Thé H, et al. Oxidative stress-induced assembly of PML nuclear bodies controls sumoylation of partner proteins. *J Cell Biol*. 2014; 204(6):931–945. [PubMed: 24637324]
26. Sahin U, Lallemand-Breitenbach V, de Thé H. PML nuclear bodies: regulation, function and therapeutic perspectives. *J Pathol*. 2014; 234(3):289–291. [PubMed: 25138686]
27. Daviter, T, Fronzes, R. Protein Sample Characterization. In: Williams, MA, Daviter, T, editors. *Protein-Ligand Interactions: Methods and Applications*. Vol. 1008. Humana Press; New York: 2013. 35–62.
28. Barysch SV, Dittner C, Flotho A, Becker J, Melchior F. Identification and analysis of endogenous SUMO1 and SUMO2/3 targets in mammalian cells and tissues using monoclonal antibodies. *Nat Protoc*. 2014; 9(4):896–909. [PubMed: 24651501]
29. Whelan SA, He J, Lu M, Souda P, Saxton RE, Faull KF, Whitelegge JP, Chang HR. Mass spectrometry (LC-MS/MS) identified proteomic biosignatures of breast cancer in proximal fluid. *J Proteome Res*. 2012; 11(10):5034–5045. [PubMed: 22934887]
30. Carazzolle MF, de Carvalho LM, Slepicka HH, Vidal RO, Pereira GAG, Kobarg J, Meirelles GV. IIS—Integrated Interactome System: a web-based platform for the annotation, analysis and visualization of protein-metabolite-gene-drug interactions by integrating a variety of data sources and tools. *PLoS One*. 2014; 9(6):e100385. [PubMed: 24949626]

31. Shannon P, Markiel A, Ozier O, Baliga NS, Wang JT, Ramage D, Amin N, Schwikowski B, Ideker T. Cytoscape: a software environment for integrated models of biomolecular interaction networks. *Genome Res.* 2003; 13(11):2498–2504. [PubMed: 14597658]
32. Hendriks IA, D'Souza RCJ, Yang B, Verlaan-de Vries M, Mann M, Vertegaal ACO. Uncovering global SUMOylation signaling networks in a site-specific manner. *Nat Struct Mol Biol.* 2014; 21(10):927–936. [PubMed: 25218447]
33. Pestov DG, Strezoska Z, Lau LF. Evidence of p53-Dependent Cross-Talk between Ribosome Biogenesis and the Cell Cycle: Effects of Nucleolar Protein Bop1 on G1/S Transition. *Mol Cell Biol.* 2001; 21(13):4246–4255. [PubMed: 11390653]
34. Hölzel M, Rohrmoser M, Schlee M, Grimm T, Harasim T, Malamoussi A, Gruber-Eber A, Kremmer E, Hiddemann W, Bornkamm GW, et al. Mammalian WDR12 is a novel member of the Pes1–Bop1 complex and is required for ribosome biogenesis and cell proliferation. *J Cell Biol.* 2005; 170(3):367–378. [PubMed: 16043514]
35. Michalec-Wawiora B, Wawiora L, Derylo K, Krokowski D, Boguszewska A, Molestak E, Szajwaj M, Tchorzewski M. Molecular behavior of human Mrt4 protein, MRTO4, in stress conditions is regulated by its C-terminal region. *Int J Biochem Cell Biol.* 2015; 69:233–240. [PubMed: 26494001]
36. Ma L, Aslanian A, Sun H, Jin M, Shi Y, Yates JR, Hunter T. Identification of small ubiquitin-like modifier substrates with diverse functions using the *Xenopus* egg extract system. *Mol Cell Proteomics.* 2014; 13(7):1659–1675. [PubMed: 24797264]
37. dos Santos MT, Trindade DM, Gonçalves K de A, Bressan GC, Anastassopoulos F, Yunes JA, Kobarg J. Human stanniocalcin-1 interacts with nuclear and cytoplasmic proteins and acts as a SUMO E3 ligase. *Mol Biosyst.* 2011; 7(1):180–193. [PubMed: 21042649]
38. Golebiowski F, Matic I, Tatham MH, Cole C, Yin Y, Nakamura A, Cox J, Barton GJ, Mann M, Hay RT. System-wide changes to SUMO modifications in response to heat shock. *Sci Signal.* 2009; 2(72):ra24. [PubMed: 19471022]
39. Bressan GC, Silva JC, Borges JC, Dos Passos DO, Ramos CHI, Torriani IL, Kobarg J. Human regulatory protein Ki-1/57 has characteristics of an intrinsically unstructured protein. *J Proteome Res.* 2008; 7(10):4465–4474. [PubMed: 18788774]
40. Lee Y, Hsieh W, Chen L, Li C. Protein arginine methylation of SERBP1 by protein arginine methyltransferase 1 affects cytoplasmic/nuclear distribution. *J Cell Biochem.* 2012; 113:2721–2728. [PubMed: 22442049]
41. Kurki S, Latonen L, Laiho M. Cellular stress and DNA damage invoke temporally distinct Mdm2, p53 and PML complexes and damage-specific nuclear relocalization. *J Cell Sci.* 2003; 116(Pt 19): 3917–3925. [PubMed: 12915590]
42. Seker H, Rubbi C, Linke SP, Bowman ED, Garfield S, Hansen L, Borden KLB, Milner J, Harris CC. UV-C-induced DNA damage leads to p53-dependent nuclear trafficking of PML. *Oncogene.* 2003; 22(11):1620–1628. [PubMed: 12642865]
43. Flick K, Kaiser P. Proteomic revelation: SUMO changes partners when the heat is on. *Sci Signal.* 2009; 2(81):pe45. [PubMed: 19638612]

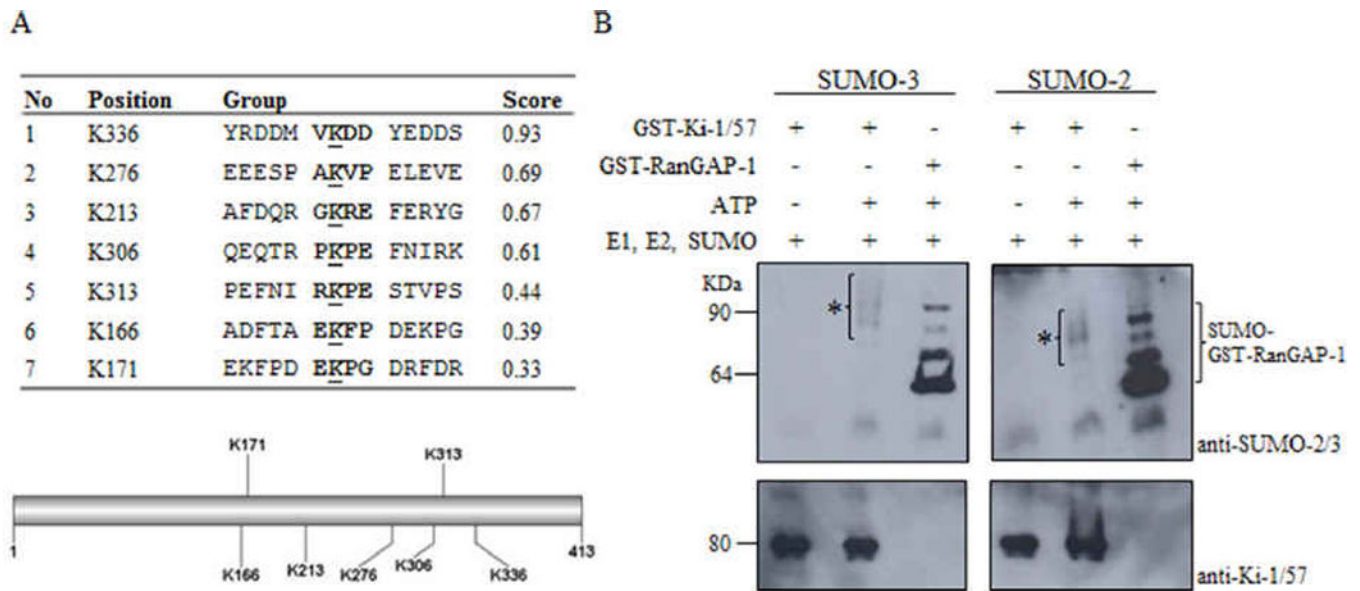


Figure 1. Ki-1/57 possesses predicted SUMOylation sites in its amino acids sequence and is modified by SUMO-2/3 *in vitro*

(A) Identification of seven potential SUMO attachment sites in the Ki-1/57 amino acid sequence through the web-available SUMOplot™ tool. Upper: Table showing the position of the potential SUMOylated lysines, its motifs (bold), lysines (underlined) and respective scores. Lower: Representation of the position of potential SUMOylated lysines in the Ki-1/57 protein. (B) *In vitro* SUMOylation assay. For *in vitro* SUMOylation assay, GST-fused Ki-1/57 (GST-Ki-1/57) was used as substrate protein for the reactions, which were performed in the presence or in the absence of ATP, presence of E1, E2 and SUMO-2 or -3 proteins as indicated. GST-RanGAP-1 was used as control. Reactions were analyzed by western blot using rabbit polyclonal anti-SUMO-2/3 (BIOMOL), or mouse monoclonal anti-Ki-1/57 (A26)². Asterisks indicate SUMO-modified-GST-Ki-1/57.

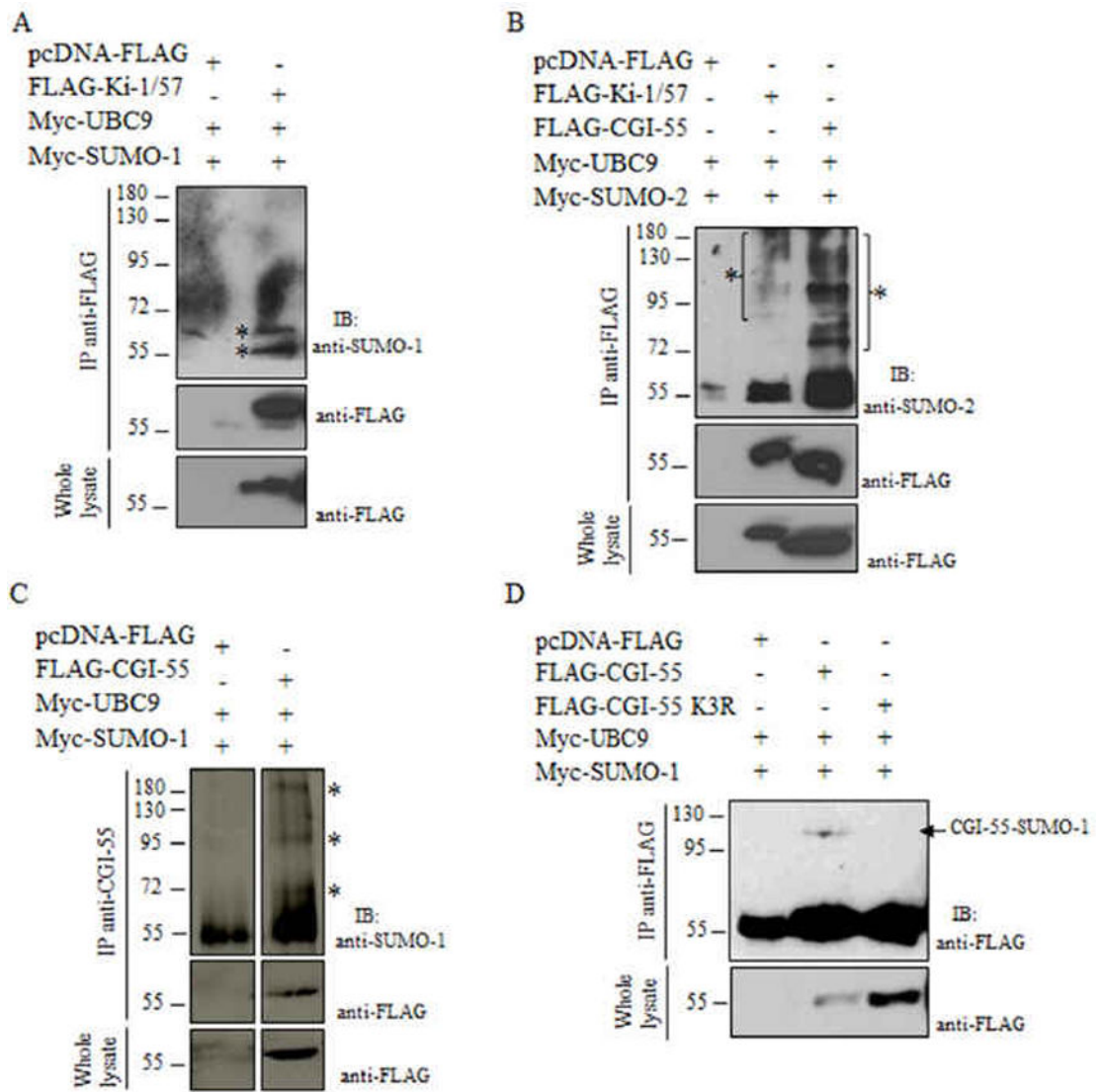


Figure 2. Ki-1/57 and its paralog, CGI-55, are conjugated with SUMO-1 and SUMO-2 proteins *in vivo*

(A) HEK293T cells were transiently co-transfected with pcDNA-FLAG (empty vector) or pcDNA6-FLAG-Ki-1/57, pcDNA3-Myc-UBC9, and pcDNA3-Myc-SUMO-1. Cells extracts were immunoprecipitated (IP) with G-sepharose beads coupled to antibody against the FLAG tag. The obtained protein complexes were analyzed by immunoblotting (IB) as indicated in the panel. Asterisk indicates SUMO-1-conjugated Ki-1/57. (B) HEK293T cells were transiently co-transfected with pcDNA-FLAG (empty vector) or pcDNA6-FLAG-Ki-1/57 or pcDNA6-FLAG-CGI-55, pcDNA3-Myc-UBC9, and pcDNA3-Myc-SUMO-1 or pcDNA3-Myc-SUMO-2. Cells extracts were immunoprecipitated (IP) with G-sepharose beads coupled to anti-FLAG antibody. The obtained protein complexes were analyzed by immunoblotting (IB) as indicated in the panel. Asterisk indicates SUMO-2-conjugated Ki-1/57 or SUMO-2-conjugated CGI-55. (C) HEK293T cells were transiently co-transfected with pcDNA-FLAG (empty vector) or pcDNA6-FLAG-CGI-55, pcDNA3-Myc-UBC9, and pcDNA3-Myc-SUMO-1. Cells extracts were immunoprecipitated (IP) with A-sepharose

beads coupled to polyclonal rabbit antibody against CGI-55. The obtained protein complexes were analyzed by immunoblotting (IB) as indicated in the panel. Asterisk indicates SUMO-1-conjugated CGI-55. (D) HEK293T cells were transiently co-transfected with pcDNA-FLAG (empty vector) or pcDNA6-FLAG-CGI-55 or pcDNA6-FLAG-CGI-55 triple mutant (K3R: K102R, K228R and K281R), pcDNA3-Myc-UBC9, and pcDNA3-Myc-SUMO-1. Cells extracts were immunoprecipitated (IP) with G-sepharose beads coupled to anti-FLAG antibody. The obtained protein complexes were analyzed by immunoblotting (IB) as indicated in the panel.

Author Manuscript

Author Manuscript

Author Manuscript

Author Manuscript

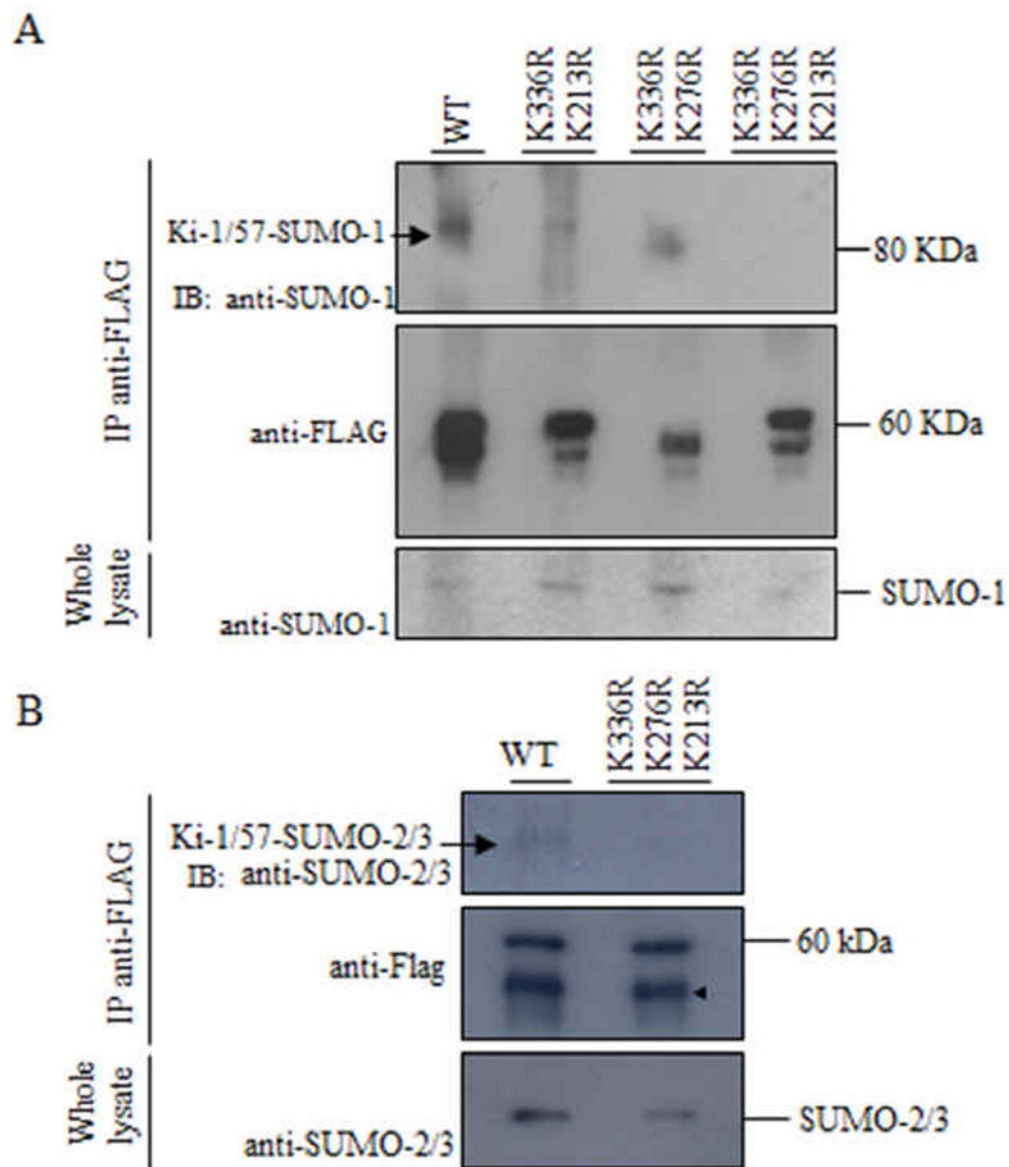


Figure 3. Ki-1/57 is SUMO-modified at lysines K213, K276 and K336

(A) HEK293T cells were transiently transfected with pcDNA6-FLAG-Ki-1/57 (wt: wild-type) or Ki-1/57 double mutants K336R/K213R or K336R/K276R or triple mutant K336R/K276R/K213R. Cells extracts were immunoprecipitated (IP) with G-sepharose beads coupled to antibody against FLAG tag. The obtained protein complexes were analyzed by western blot using anti-FLAG and anti-SUMO-1 antibodies. Arrow indicates SUMO-1-conjugated Ki-1/57. (B) HEK293T cells were transiently transfected with pcDNA6-FLAG-Ki-1/57 (wt: wild-type) or Ki-1/57 triple mutant K336R/K276R/K213R. Cells extracts were immunoprecipitated (IP) with G-sepharose beads coupled to anti-FLAG antibody. The obtained protein complexes were analyzed by western blot using anti-FLAG and anti-SUMO-2/3 antibodies. Arrow indicates SUMO-2/3-conjugated Ki-1/57. Arrowhead indicates the antibody heavy chain.

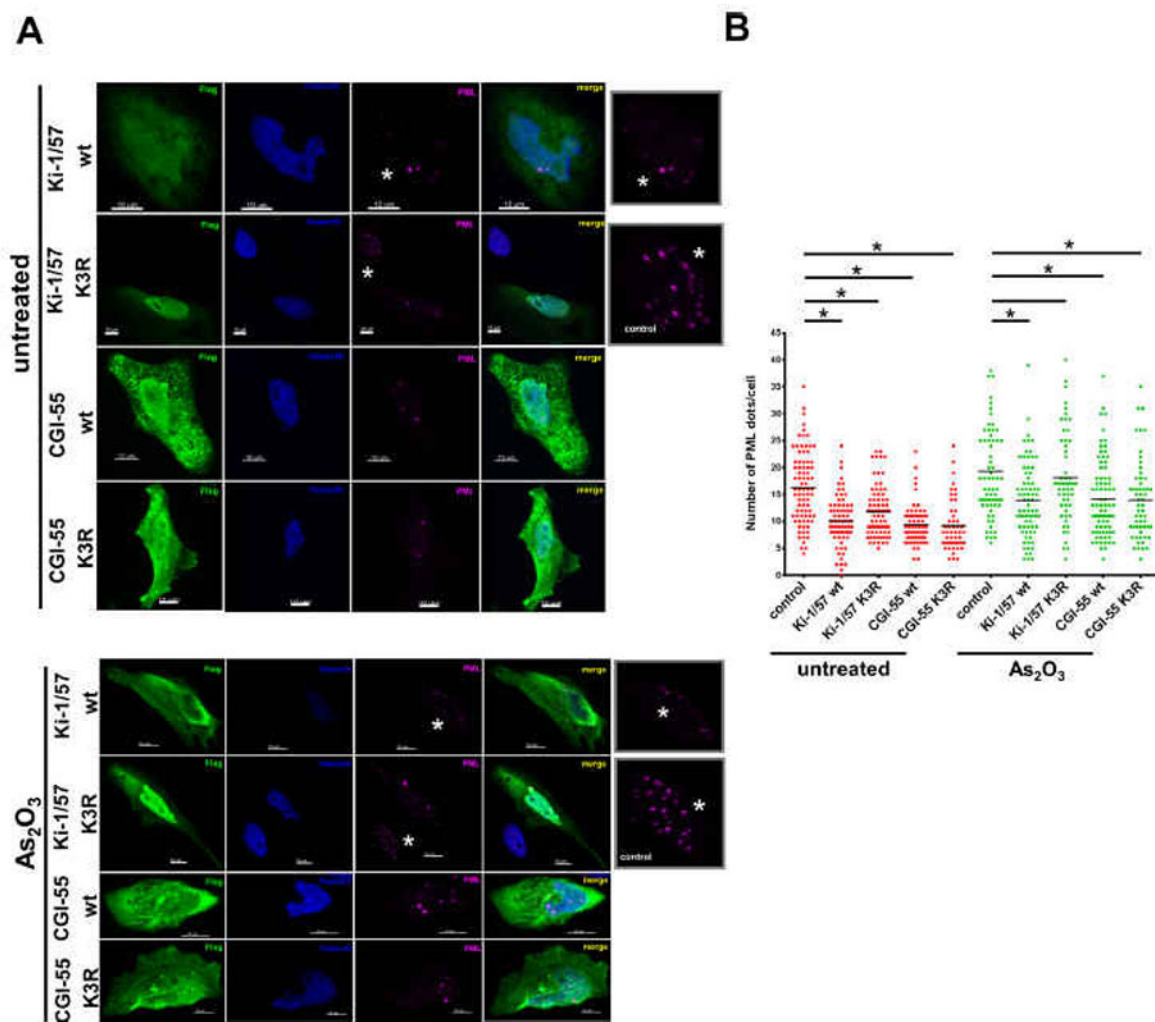
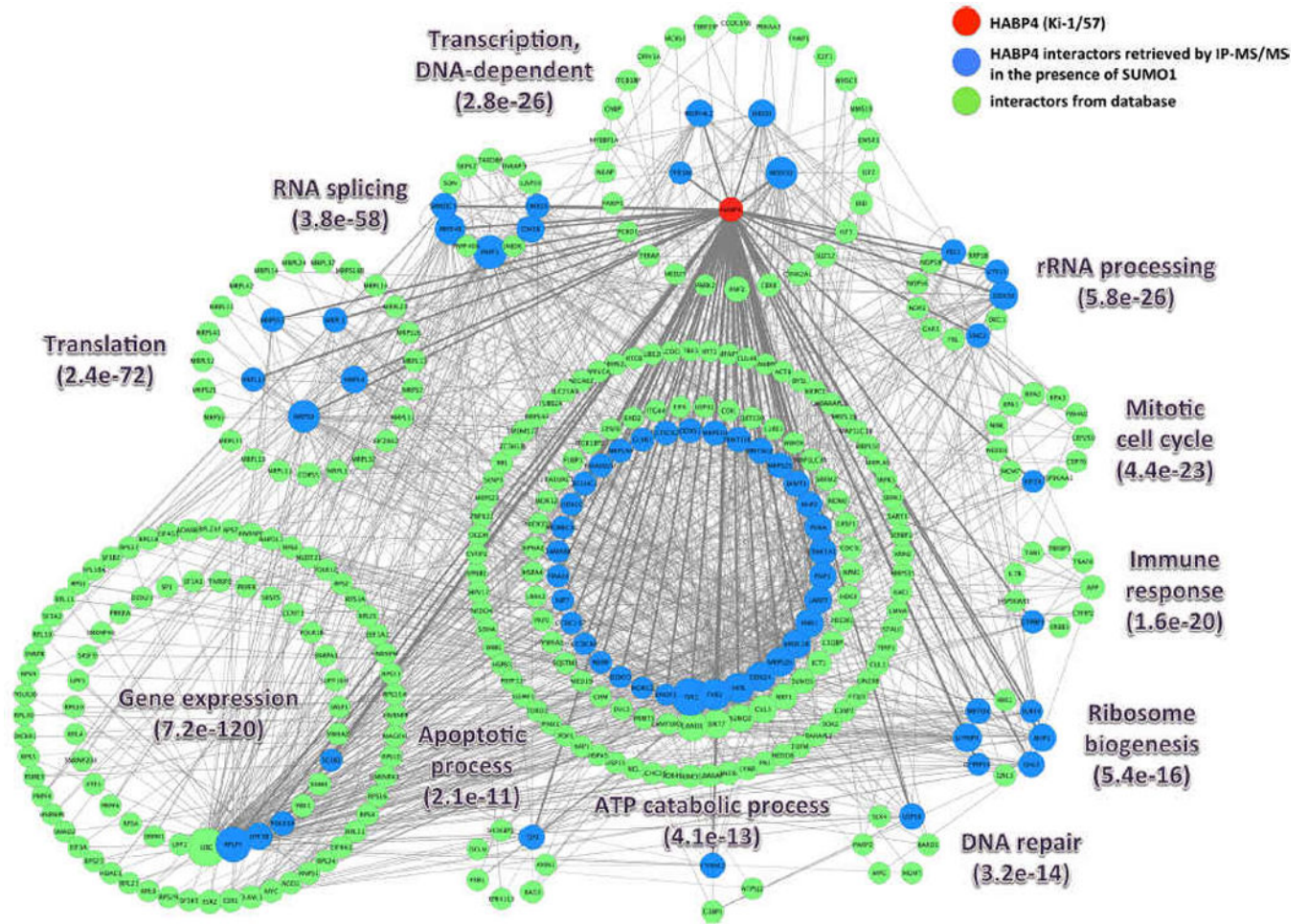


Figure 4. Ki-1/57 and CGI-55 affect PML-NBs number

(A) HeLa cells transfected with FLAG-tagged constructs as indicated were either not treated or treated with arsenic trioxide (As_2O_3) for 90 min and stained for immunofluorescence confocal microscopy using indicated antibodies. Images are depicted as maximum intensity projections (MIPs) of z-stacks throughout the cell to allow PML captures in all three dimensions. Nuclei were detected by Hoechst. Scale bars equals 10 μm . The asterisk indicates the cell shown in higher magnification in the last column. (B) PML numbers within each individual cell were determined using the Spots object on Imaris software (Bitplane) using a fixed spot size of 0.5 μm (the measured average XY diameter of nuclear bodies). Adjacent nontransfected interphase cells from the same field of view marked with an asterisk and enlarged (A) were measured in parallel and used as control. Results were calculated from > 75 cells collected from at least two independent experiments. Each dot represents a single cell. Bars represent mean values. * $P < 0.05$ by Students t-test.



Author Manuscript

Author Manuscript

Author Manuscript

Author Manuscript

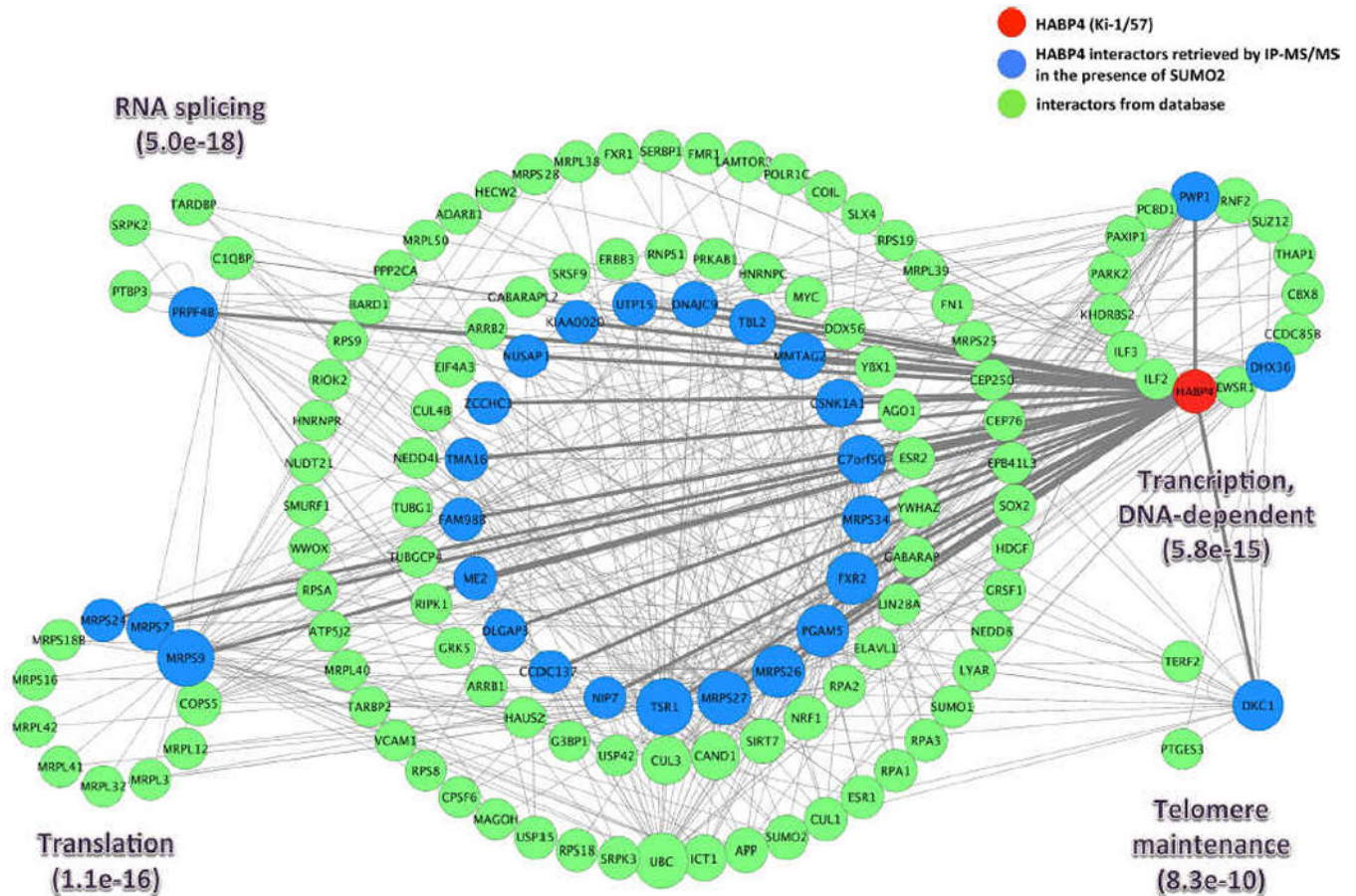


Figure 5. Interaction networks of the retrieved overexpressed Ki-1/57 (HABP4) or CGI-55 (SERBP1) interacting partners from IP-MS/MS in the presence of overexpressed SUMO1 or SUMO2

The enriched GO biological processes among the IP-MS/MS HABP4 or SERBP1 interactors (blue) and the background intermediary proteins (green) are depicted in the (A) HABP4 + SUMO1, (B) HABP4 + SUMO2, (C) SERBP1 + SUMO1 and (D) SERBP1 + SUMO2 networks by clustering the proteins involved in each of the biological processes with a circle layout. Clusters were assigned only to selected most relevant enriched biological processes containing at least three proteins with one from the IP-MS/MS data; proteins belonging to more than one biological process were assigned to clusters with the best enrichment p-values. The nodes sizes are depicted according to their connectivity degree. Thicker edges correspond to the novel interactions identified between HABP4 or SERBP1 and the IP-MS/MS proteins. The protein-protein interaction networks were built using the IIS platform and visualized using the Cytoscape software.